

## Supporting Information

# Electric Field-Enhanced Electrochemical CRISPR Biosensor for DNA Detection

Ziyue Li<sup>1,2</sup>, Xiong Ding<sup>1</sup>, Kun Yin<sup>1</sup>, Zhiheng Xu<sup>1</sup>, Kumarasen Cooper<sup>3</sup>, and Changchun Liu<sup>1,2\*</sup>

1. *Department of Biomedical Engineering, University of Connecticut Health Center, 263 Farmington Ave., Farmington, CT, 06030, United States*
2. *Department of Biomedical Engineering, University of Connecticut, 260 Glenbrook Road, Storrs, CT, 06029, United States*
3. *Department of Pathology and Laboratory Medicine, University of Pennsylvania, 3400 Spruce St. Philadelphia, PA 19104, United States*

### \* Corresponding author

Dr. Changchun Liu

Department of Biomedical Engineering

University of Connecticut Health Center

263 Farmington Avenue

Farmington, CT 06030

Phone: (860)-679-2565

E-mail: [chaliu@uchc.edu](mailto:chaliu@uchc.edu)

Multipurpose interface

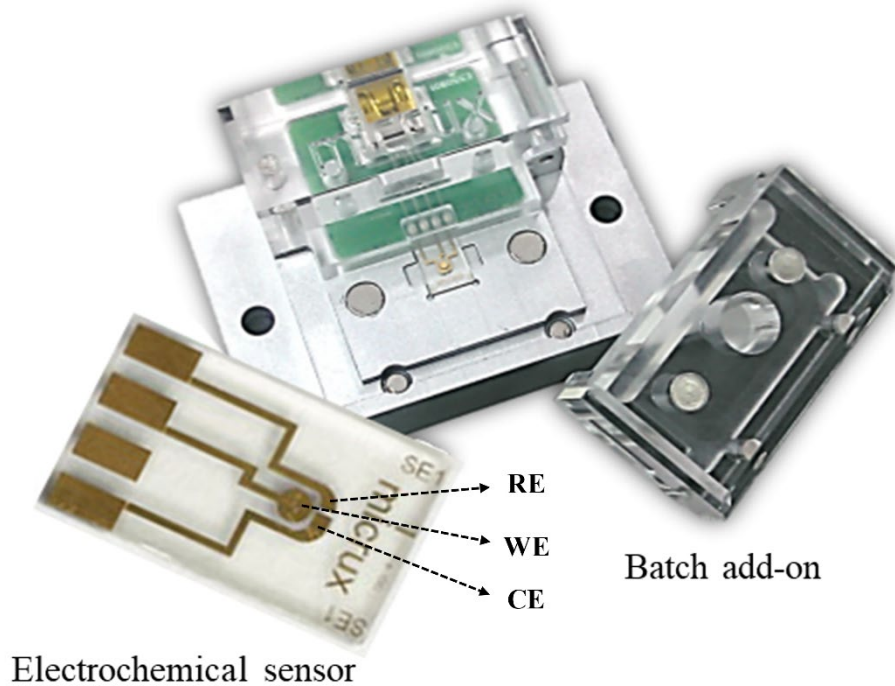


**Figure S1.** Photograph of electrochemical biosensor platform. The electrochemical platform consists of: i) multipurpose interface, ii) batch add-on and iii) electrochemical sensor.

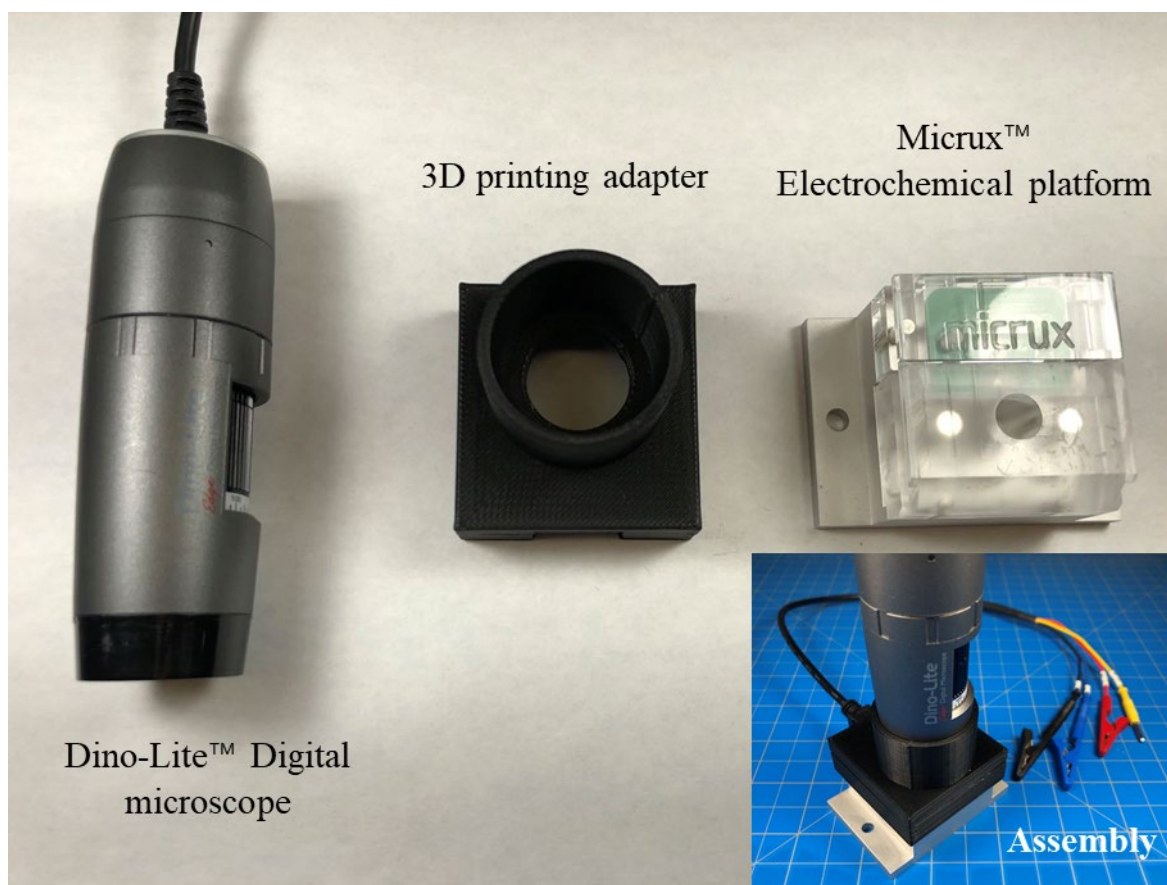


**Figure S2.** Photograph of the home-made CRISPR-based fluorescence detection platform, which is used to real-time monitor fluorescence in the electrochemical chamber.

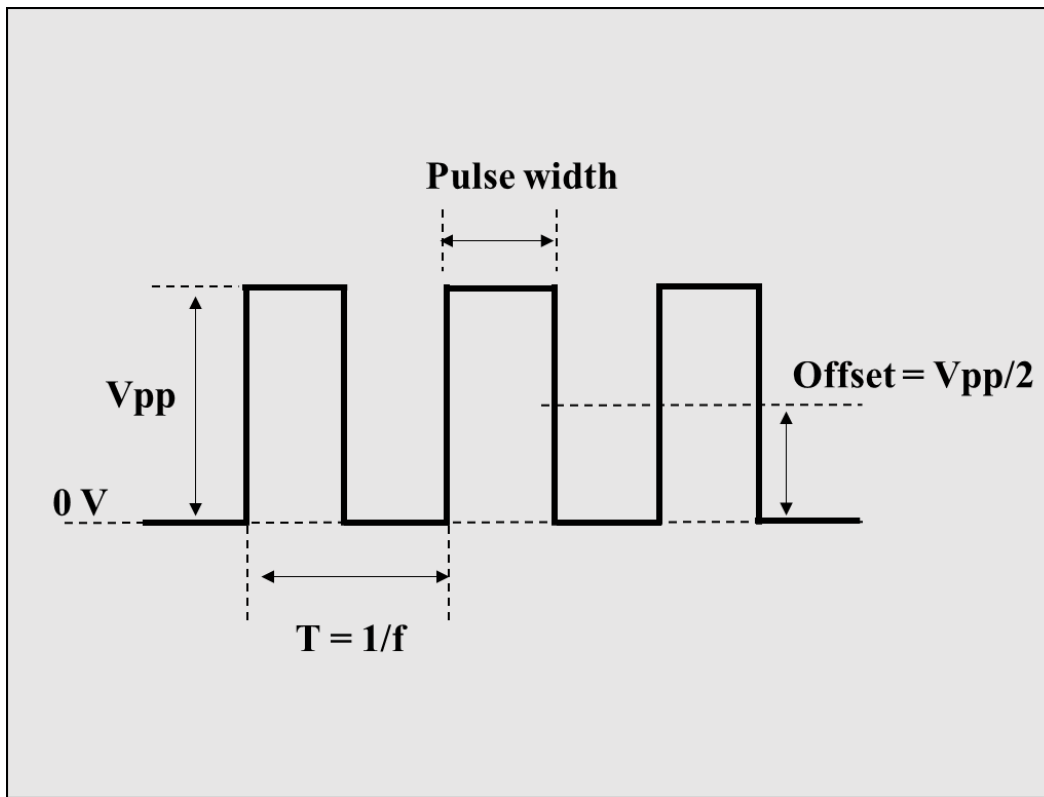


**Figure S3.** Electric field waveform. Electric field consists of an AC electric field and a DC offset. The peak-to-peak potential ( $V_{pp}$ ) is the amplitude of the electric field. The offset potential is set as the half of the  $V_{pp}$  and the pulse width is set as 50% of period ( $T$ ).

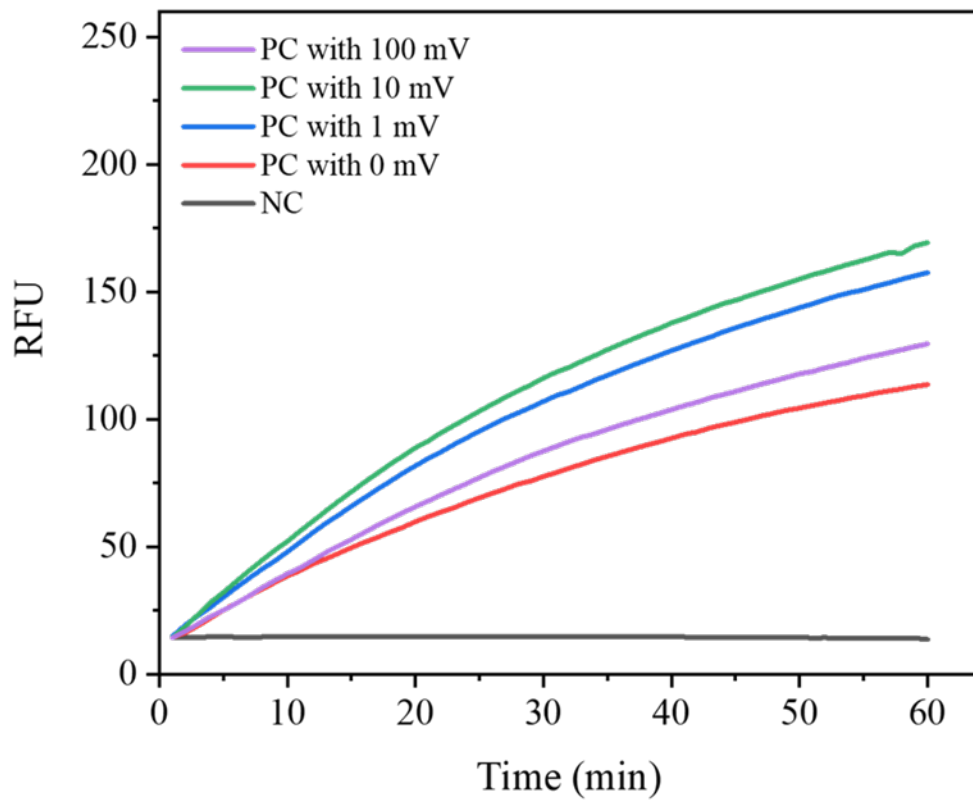


**Figure S4.** The effect of different peak-to-peak values (Vpp) ranging from 0 to 100 mV on the CRISPR-based nucleic acid detection.

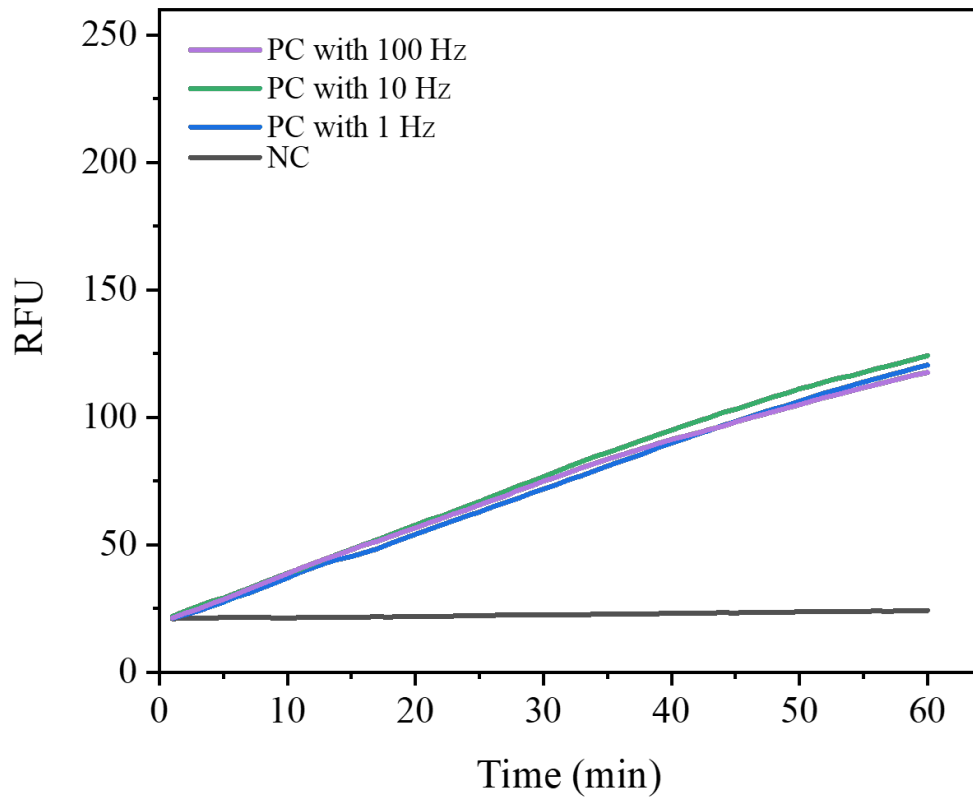


**Figure S5.** Effect of different frequency ranging from 1 to 100 Hz on the CRISPR-based nucleic acid detection.

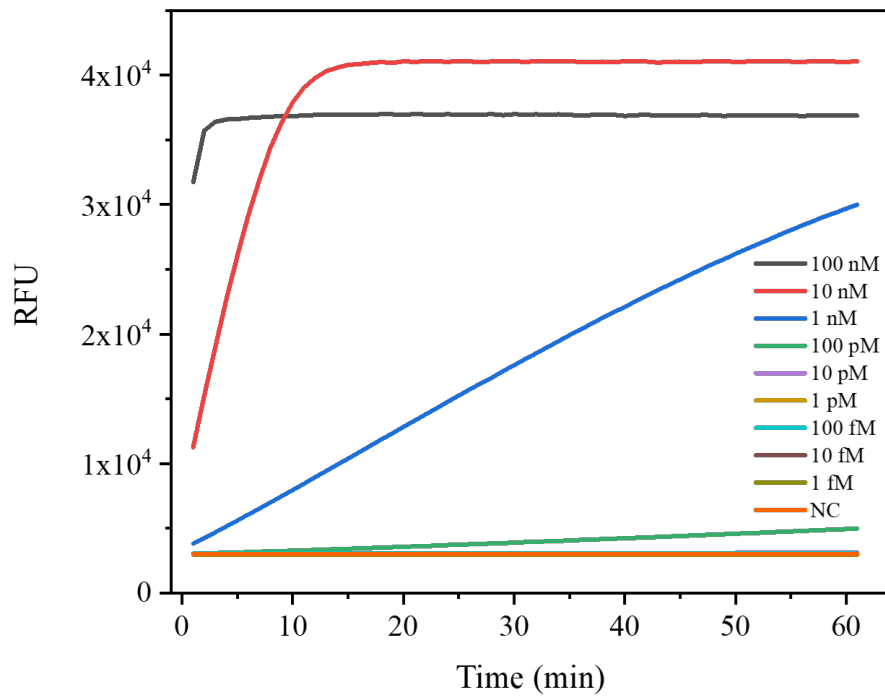


**Figure S6.** Real-time CRISPR fluorescence curves for detection of HPV-16 DNA target ranging from 1 fM to 100 nM in the reaction tubes.

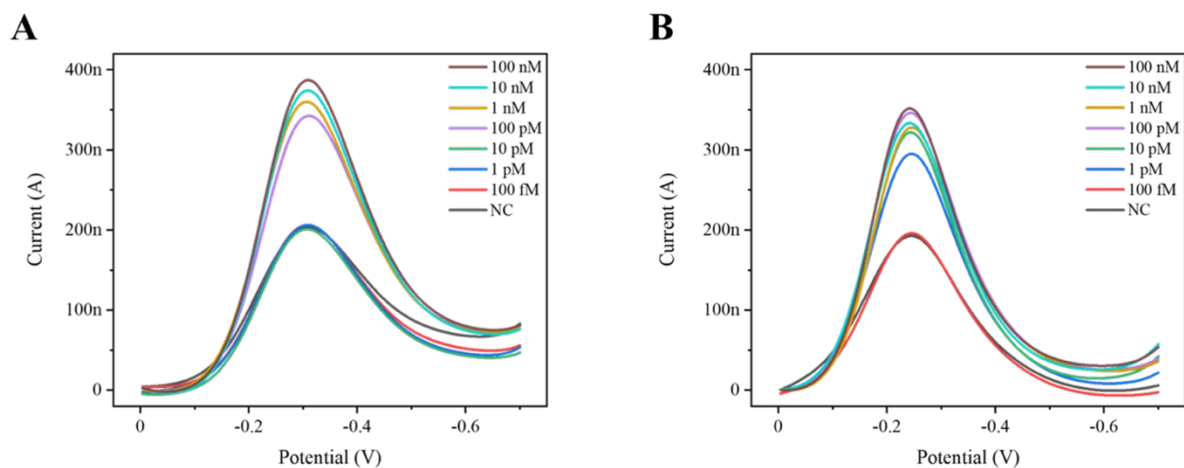


**Figure S7.** Comparison of HPV-16 DNA detection by electrochemical CRISPR biosensor with or without pulsed electric field. A) Differential pulse voltammetry (DPV) curves of electrochemical CRISPR biosensor without applying an electric field for detection of HPV-16 target ranging from 100 fM to 100 nM. B) Differential pulse voltammetry curves of electrochemical CRISPR biosensor with applying an electric field for detection of HPV-16 target ranging from 100 fM to 100 nM.



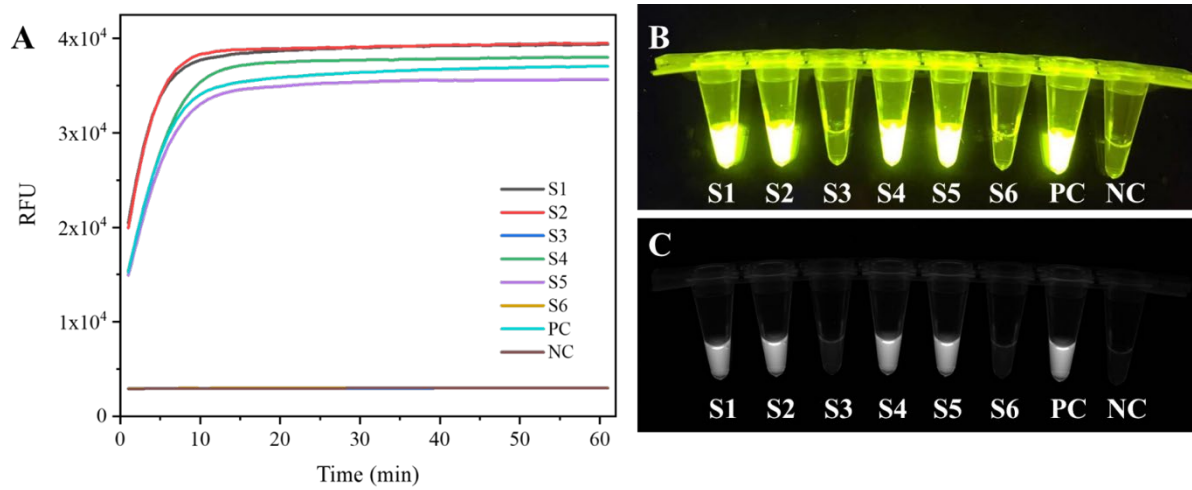


**Figure S8.** CRISPR-based fluorescence detection of HPV-16 DNA in clinical samples after RPA pre-amplification. A) Real-time fluorescence curves of CRISPR-based fluorescence detection of HPV-16 DNA. B & C) Endpoint fluorescence images of CRISPR-based reaction tube in a portable transilluminator (MaestroGen Inc.) and a ChemiDoc MP Imaging System (Bio-Rad), respectively.

**Table S1.** Related nucleic acids sequence.

<b>Oligonucleotide</b>	<b>Sequence</b>
<b>crRNA</b>	
LbCas12a-crRNA-HPV-16	UAAUUUCUACUAAGUGUAGAUUGAAGUAGAU AUGGCAGCAC
<b>Target</b>	
HPV-16 L1	ATAATGGCATTGTTGGGGTAACCAACTATTTGTTACTGTTGTTGATA CTACACGCAGTACAAATATGTCATTATGTGCTGCCATATCTACTTCAG AAACTACATATAAAAATACTAACTTTAAGGAGTACCTACGACATGGG GAGGAATATGATTT
<b>RPA Primers</b>	
FP HPV16 L1	TTGTTGGGGTAACCAACTATTTGTTACTGTT
RP HPV16 L1	CCTCCCCATGTCTGAGGTACTCCTTAAAG
<b>Reporter</b>	
ssDNA-FQ	/56-FAM/TTATT/3IABkFQ/
ssDNA-MB	TTA TT/3MeBIN/